

# Geodesic acoustic mode test of the 2DX code

D. A. Baver and J. R. Myra

*Lodestar Research Corporation, Boulder Colorado 80301*

Maxim Umansky

*Lawrence Livermore National Laboratory*

## 1 Introduction

This test was devised to verify the ability of the 2DX eigenvalue code to correctly solve a simple fluid model relevant to edge turbulence in tokamaks. Since the functionality of the 2DX code depends on both the source code itself and the input file defining the system of equations to solve (structure file), this test demonstrates both. Since a similar test was performed on an earlier version of 2DX, this verifies that the current version retains this functionality. Moreover, since the structure file for this test represents a subset of a more general 6-field model, many of the terms in that test are also verified.

This test compares 2DX results to approximate analytic solutions for relevant eigenmodes of interest.

## 2 Description

### 2.1 Code structure

The 2DX code is a highly flexible eigenvalue solver designed for problems relevant to edge physics in toroidal plasma devices. Its flexibility stems from the use of a specialized input file containing instructions on how to set up a particular set of equations. Because of this, the 2DX code permits model equations to be changed without altering its source code. The drawback to this approach is that any change to the structure file represents a potential source of error, necessitating re-verification. This problem is offset by the fact that the source code remains unchanged, thus testing one structure file builds confidence in the underlying code that interprets the structure file. Also, structure files can be translated into analytic form, thus allowing the user to verify that the file contains the equations intended.

The structure file contains two main parts: an elements section, which constructs the differential operators and other functions used in a particular set

of equations, and a formula section, which assembles these into an actual set of equations. This separation means that elements can be recycled in other structure files. By testing one structure file, one builds confidence in the elements used in that file. The main source of error when switching to a different structure file then is in the formula section, which can be manually verified by translating into analytic form.

Regardless of the content of the structure file, the 2DX code is fundamentally a finite-difference eigenvalue solver. As such, it is subject to the limitations of any code of its type.

## 2.2 Model equations

For this test we use the following model equations [1]:

$$\gamma \nabla_{\perp}^2 \delta \Phi = + \frac{2B}{n} C_r \delta p - \frac{B^2}{n} \partial_{\parallel} \nabla_{\perp}^2 \delta A + \Gamma \nabla_{\perp}^2 \delta \Phi + \mu_{ii} \nabla_{\perp}^4 \delta \Phi \quad (1)$$

$$\gamma \delta n = \frac{2}{B} (C_r \delta p_e - n C_r \delta \Phi) - n \partial_{\parallel} \delta u - \partial_{\parallel} \nabla_{\perp}^2 \delta A \quad (2)$$

$$\gamma \delta u = - \frac{1}{n} \nabla_{\parallel} \delta p \quad (3)$$

$$- \gamma \nabla_{\perp}^2 \delta A = \nu_e \nabla_{\perp}^2 \delta A - \mu n \nabla_{\parallel} \delta \Phi + \mu T_e \nabla_{\parallel} \delta n \quad (4)$$

$$\delta p = (T_e + T_i) \delta n + n (\delta T_e + \delta T_i) \quad (5)$$

$$C_r = \mathbf{b} \times \kappa \cdot \nabla = -\kappa_g R B_p \partial_x + i(\kappa_n k_b - \kappa_g k_{\psi}) \quad (6)$$

$$\nabla_{\perp}^2 = -k_b^2 - jB(k_{\psi} - i\partial_x R B_p)(1/jB)(k_{\psi} - iR B_p \partial_x) \quad (7)$$

$$\partial_{\parallel} Q = B \nabla_{\parallel} (Q/B) \quad (8)$$

$$\nabla_{\parallel} = j \partial_y \quad (9)$$

$$\delta v_E \cdot \nabla Q = -i \frac{k_z (R B_p \partial_x Q)}{B} \delta \Phi \quad (10)$$

$$\nu_e = .51 \nu_r n / T_e^{3/2} \quad (11)$$

## 2.3 Boundary conditions

This test case uses phase-shift periodic boundary conditions in the parallel direction, and zero-derivative boundary conditions in the radial direction. The phase shift in the parallel direction is given by:

$$e^{i2\pi n q} \quad (12)$$

## 2.4 Profile setup

The formulas in Eq. 1-4 are normalized to Bohm units. Values are converted by dividing input distances by  $\rho_s$ , and input magnetic fields are in Tesla. Output eigenvalues are multiplied by  $\omega_{ci}$ . Resistivity is given by the formula:

$$\nu_r = \frac{\mu}{.51\sigma} \quad (13)$$

where

$$\sigma = 1.96 \frac{\omega_{ce}}{\nu_{ei}} \quad (14)$$

The geometry used is a thin toroidal annulus with major radius  $R$ . Other geometric effects are neglected, so that the domain is effectively a shearless slab. Both normal and geodesic curvature are calculated as follows:

$$\kappa_n = \frac{\cos(y)}{R} \quad (15)$$

$$\kappa_g = \frac{\sin(y)}{R} \quad (16)$$

Parallel derivatives are calculated using the Jacobian factor  $1/qR$ . Toroidal mode number is set to zero. Binormal wavenumber is therefore also equal to zero. In addition, a constant parameter  $\Gamma$  is used to give the GAM a positive growth rate; physically, this represents nonlinear drive of the GAM by turbulence.

## 3 Analytic results

Since the eigenmodes of the GAM model are not homogenous, there is no exact analytic solution. An approximate solution can be found by assuming that  $\delta A$  terms are small and that geodesic curvature has the form  $\kappa_g = \hat{\kappa}_g \sin \theta \mathbf{e}_\theta$ . For purposes of this calculation, we normalize  $n$  and  $T$  to reference values, set  $\mu_{ii}$  to zero, and set the Jacobian factor  $j = 1/qR$ . This results in the following dispersion relation:

$$i\omega(\omega^2 - \omega_g^2) = -\Gamma(\omega^2 - \omega_s^2) \quad (17)$$

where

$$\omega_s = k_{\parallel} c_s \quad (18)$$

$$\omega_g^2 = \frac{c_s^2}{R^2} \left( 2 + \frac{1}{q^2} \right) \quad (19)$$

If  $\Gamma$  is small, this yields a frequency and growth rate:

$$\omega = \omega_g + \frac{i\Gamma}{2 + 1/q^2} \quad (20)$$

In addition, there is also a zero frequency mode which can be identified as a zonal flow. This has a growth rate:

$$\omega = \frac{i\Gamma}{1 + 2q^2} \quad (21)$$

These approximations break down at certain specific values of  $q$ . This occurs because of a resonance between the GAM and spatial harmonics of the sound wave. The sound wave has frequency:

$$\omega_s = \frac{m^2}{q^2 R^2} \quad (22)$$

Consequently, a resonance between  $\omega_s$  and  $\omega_g$  occurs at values of  $q$  that satisfy the equation:

$$q = \sqrt{\frac{m^2 - 1}{2}} \quad (23)$$

## 4 Numerical results

The code was tested by sweeping the variable  $q$  and plotting the fastest growing eigenvalue. The parameters used in this test are as follows:

$\rho_s = 1$   
 $R = 1000$   
 $\delta a = 100$   
 $n = 1$   
 $T_e = 1$   
 $T_i = 0$   
 $\delta_{er} = 1$   
 $\mu = 1836$   
 $k_\psi = .2$   
 $\Gamma = .00001$   
 $B = 1$   
 $RB_p = 1$   
 $\omega_{ci} = 1$

A more complete list of input values is shown in table 1.

The results of this test are shown in Fig. 1. The raw data is also shown in table 2. The red line is the growth rate predicted for the zonal flow mode, whereas the yellow line is the growth rate predicted for the analytic GAM. The blue line is the 2DX result. Note that the 2DX result agrees with whichever of the two analytic results is greater, except at certain specific  $q$  values. These values agree with those predicted by the formula in Eq. 23.

## References

- [1] N. Winsor, J.L. Johnson and J.M. Dawson, Phys. Fluids **11**, 2448 (1968).

nx	4	ny	32
dx	33.3333	dy	.202683
$\omega_{ci}$	1	n	0
$\mu$	1836	$\nu_r$	.0000196078
q	$q_0$	$k_b$	0
$j$	$.001/q_0$	$k_\psi$	.2
$\kappa_n$	$.001 \cos(y)$	$\kappa_g$	$.001 \sin(y)$
B	1	$RB_p$	1
$n_0$	1	$T_e$	1
$\Gamma$	.00001		

Table 1: Non-dimensional profile functions and parameters used in the GAM test case, as a function of  $q_0$ .

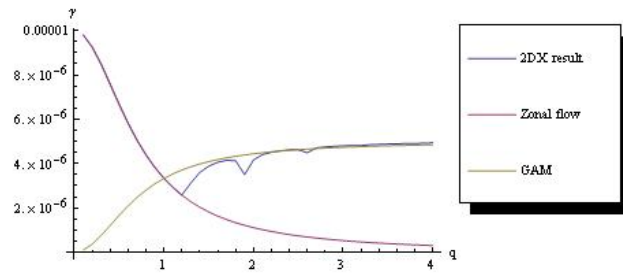


Figure 1: Growth rate vs.  $q$  for the GAM model.

q	$\gamma \times 10^6$	Zonal flow	Analytic GAM	q	$\gamma \times 10^6$	Zonal flow	Analytic GAM
.1	9.80481	9.80392	.098039	2.1	4.41140	1.01833	4.49084
.2	9.26424	9.25926	.370370	2.2	4.51496	.936330	4.53184
.3	8.48054	8.47458	.762712	2.3	4.57988	.863558	4.56822
.4	7.58423	7.57576	1.21212	2.4	4.62225	.798722	4.60064
.5	6.67693	6.66667	1.66667	2.5	4.62246	.740741	4.62963
.6	5.82520	5.81395	2.09302	2.6	4.49110	.688705	4.65565
.7	5.06206	5.05051	2.47475	2.7	4.70994	.641849	4.67908
.8	4.39735	4.38596	2.80702	2.8	4.75274	.599520	4.70024
.9	3.82771	3.81579	3.09160	2.9	4.78082	.561167	4.71942
1.0	3.34361	3.33333	3.33333	3.0	4.80332	.526316	4.73684
1.1	2.93355	2.92398	3.53801	3.1	4.81994	.494560	4.75272
1.2	2.58617	2.57732	3.71134	3.2	4.81926	.465549	4.76723
1.3	3.12899	2.28311	3.85845	3.3	4.85264	.438982	4.78051
1.4	3.60623	2.03252	3.98374	3.4	4.86981	.414594	4.79270
1.5	3.88574	1.81818	4.09091	3.5	4.88342	.392157	4.80392
1.6	4.06130	1.63399	4.18301	3.6	4.89546	.371471	4.81426
1.7	4.15147	1.47493	4.26254	3.7	4.90607	.352361	4.82382
1.8	4.13123	1.33690	4.33155	3.8	4.91024	.334672	4.83266
1.9	3.50439	1.21655	4.39173	3.9	4.92539	.318269	4.84087
2.0	4.16704	1.11111	4.44444	4.0	4.93414	.303030	4.84848

Table 2: Growth rate vs. q for the GAM model.